Control of mesoporous and crystalline structures in turbostratic carbon derived from Fe- or Ni-doped phenolic resin

Katsuya Inomata · Yoshinobu Otake

Abstract A technique to control the mesoporous structure and crystallites present in turbostratic carbon (Ts-carbon) derived from Fe- and Ni-doped phenolic resin is described. To eliminate the effect of heat treatment temperature, all of the Fe- and Ni-doped phenolic resins are carbonized at a fixed temperature of 1000 °C. The catalyst content in the obtained Ts-carbon varies from 0.001 to 5 mmol/g. Mesopores and turbostratic crystallites are formed in the Ts-carbon samples, and these increase in size as the catalyst content and its particle size increases. The turbostratic crystallites assemble to form carbon aggregates with a cup-stacked, thin tube-like, or coil-like structure. The mesopore surface area increases proportionally with the amount of turbostratic crystallites rather than the type of carbon aggregate. It is proposed that the mesopore is surrounded by turbostratic crystallites. Altering the size of the turbostratic crystallites in Ts-carbon has revealed an effective method for controlling the size and volume of its mesopores.

Introduction

The importance of mesoporous structures has been recognized, and mesoporous carbon has been applied in the adsorption of large molecules such as dioxin and vitamins [1–3] and in electric double layer capacitors [4]. Activation is widely used to create mesopores in carbon [1, 5–7]. However, during the activation process substantial mass loss takes place so the obtained mesoporous carbon is fragile. Recent studies have shown that mesoporous carbon can be prepared via catalytic graphitization without activation [8–12], providing an alternative method to facilitate the formation of mesoporous carbon.

Catalytic graphitization is a solid-state catalytic reaction of carbon. Carbonization of a carbon precursor with a metallic compound catalyzes the conversion of carbon with an amorphous structure into graphite and turbostratic crystallites. Turbostratic carbon (Ts-carbon), which consists predominantly of turbostratic crystallites, is reported to possess mesopores [8–12]. Ts-carbon also exhibits a highly crystalline structure and high electronic conductivity [13, 14]. Thus, Ts-carbon has shown excellent catalytic activity for H_2S decomposition [15], methanol electrooxidation [16, 17], and oxygen reduction [18]. Moreover, turbostratic crystallites in Ts-carbon are clustered together to form aggregates that can possess tube-like and coil-like structures [8, 16, 19]. These carbon aggregates show superior features to nanocarbon samples prepared in the gas phase [16]. Because of these unique features, Ts-carbon possesses some advantages over conventional porous carbon with an amorphous structure. As such, there is a growing interest in controlling the formation of mesoporous structures in Ts-carbon.

The porosity of Ts-carbon was first noted in 1981 [20], but about 20 years passed before further studies were performed. In 2000, the existence of mesopores in Ts-carbon was first discovered. Maldonado-Hodar et al. [10] revealed that Ts-carbon contained mesopores with a wide range of pore sizes from micro- to macropores. Hatori et al. [11] suggested that the development of mesoporous structures was related to the growth of metal particles. Conversely, Zhao et al. [12] proposed that the mesopores were derived from interspaces between the carbon aggregates. The location of the mesopores in Ts-carbon remains

K. Inomata (✉) · Y. Otake
Department of Applied Chemistry, Meiji University, 1-1-1
Higashimita, Tama-ku, Kawasaki, Kanagawa 214-8571, Japan
e-mail: ino@isc.meiji.ac.jp

unclear. Consequently, control over the size of mesopores in Ts-carbon has not been accomplished.

Oya et al. [20] reported that the developed porosity of Ts-carbon was attributed to the presence of turbostratic crystallites, because carbons with more or less ordered crystallites do not exhibit such porosity. Recently, we showed that altering the size of turbostratic crystallites possibly controls the size of mesopores in Ts-carbon [8]. These reports suggest that the formation of mesopores in Ts-carbon is related to the turbostratic crystallites. Thus, the ability to control the size of turbostratic crystallites in Ts-carbon is needed to produce controlled mesopores in Ts-carbon.

Altering the size of turbostratic crystallites has been accomplished by heat treatment at elevated temperature [14, 21–23]. The elevated temperature also causes sintering, which leads to enlargement of the catalyst particles [24, 25]. The size of the catalyst particle is believed to be another factor that causes structural changes in turbostratic crystallites [23, 26, 27]. However, this relationship remains unclear because the effects of the size of the catalyst and the heat treatment temperature have not been studied separately. The objective of this study is to investigate the correlation between the sizes of the catalyst and turbostratic crystallites to allow control over the formation of mesoporous structures in Ts-carbon. The size of the catalyst is altered by changing the amount added, and then carbonizing at a fixed heat treatment temperature of 1000 °C to eliminate the effect of the temperature. Phenolic resin is used as the carbon precursor, and its carbonization is catalyzed by Fe or Ni, which are widely used as catalytic graphitization catalysts [8–28]. To vary the size of the catalyst over a wide range, the catalyst loading is performed by two different methods. The sizes of the catalyst and turbostratic crystallites are estimated by X-ray diffraction (XRD) and transmission electron microscope (TEM) studies, while the porous structure of the resulting Ts-carbon is evaluated by N_2 adsorption/desorption measurements.

Experimental

Sample preparation

Fe- and Ni-containing carbon samples were synthesized from phenolic resin (resol-type phenol formaldehyde resin, Gun Ei Chemical Industry Co, Ltd, Japan) containing ferrocene or nickelocene (Kanto Chemical Co, Inc, Japan). The phenolic resin and metallic compounds were mixed in two ways: by homogeneous mixing in methanol (method A), or by mechanical mixing using an agate mortar (method B).

Method A is conventionally employed in studies relating to Ts-carbon, and was used by us previously [8]. Designated amounts of ferrocene or nickelocene were dissolved in methanol and then added to a solution of phenolic resin in methanol. Each phenolic resin solution containing a metallic compound was heated until the methanol evaporated and then thermoset for 10 days at 80 °C. Consequently, the metallic compound can be homogeneously dispersed in the phenolic resin. However, it was difficult to prepare homogeneous mixtures when the content of nickelocene was high. Thus, nickel nitrate hexahydrate (Kanto Chemical Co, Inc, Japan) was used as an alternative to nickelocene when the required nickel content was greater than 0.35 mmol/g.

Method B consisted of mechanical mixing of the metallic compounds and phenolic resin. First, the phenolic resin was thermoset for 10 days at 80 °C and subsequently ground into fine particles. These were then mixed with a designated amount of ferrocene or nickelocene using an agate mortar.

The obtained phenolic resins containing Fe or Ni catalyst were subjected to carbonization with fixed heat treatment conditions. The resins were heated to 1000 °C at a constant heating rate of 5 °C/min, and then maintained at this temperature for 1 h under a flow of high-purity Ar. The catalyst content in the obtained carbon samples was adjusted so that the resins carbonized at 1000 °C contain 0.001–5 mmol/g of metallic Fe or Ni. The carbon samples thus obtained are named according to their metal content, metal species, and mixing method, for example, 0.759 Fe-A and 0.0240 Ni-B. The carbon sample produced without addition of any metallic compounds is termed PF.

Characterization

The Fe and Ni content in the samples carbonized at 1000 °C were estimated from their ash. The crystalline state of the turbostratic crystallites and Fe and Ni catalyst were evaluated by XRD (Rigaku, Rint1200) with Cu-Kα radiation. In this study, the carbon crystal thickness (L_c) is used as an index value of the size of the turbostratic crystallites. In the measurement of L_c, high-purity silicon (Silicon powder 640c, NIST) was used as an internal standard. L_c was calculated using the program Carbon Analyzer Version 3.51; details of the correction and calculations have been reported previously [29, 30]. The size of the catalyst particles was estimated using TEM (JEOL, JEM-2100F) and XRD. TEM was also used to observe nanoscale structure of the Ts-carbon. N_2 adsorption/desorption measurements were carried out at 77 K using a Belsorp 18 plus analyzer (BEL, Japan). The volume, size distribution, and surface area of the mesopores were estimated using the Barrett−Joyner−Halenda (BJH) method [31].

Results and discussion

XRD profiles of the carbon samples formed with or without metal catalyst are shown in Fig. 1. Adding Fe and Ni catalyst resulted in the appearance of a sharp peak at 2θ of around 26°. This peak is attributed to the formation of turbostratic crystallites. As the content of catalyst increased, the intensity of this peak increased. This means the proportion of turbostratic crystallites increased with the catalyst content. In the profiles of Fe-A and Fe-B, diffraction peaks corresponding to α-Fe (at $2\theta = 44.6°$) and γ-Fe (at $2\theta = 43.6°$ and 51.0°) were detected. Although γ-Fe is thermodynamically stable above 911 °C according to the Fe–C phase diagram [32], the γ-Fe phase was found in the carbon samples at ambient temperature. The presence of γ-Fe in Ts-carbon has also been reported in previous studies [18, 24, 25, 33]. Ozaki et al. [33] suggested that dissolution of carbon into γ-Fe reduced the phase transition temperature. The dissolution of carbon into metals plays an important role in the formation of turbostratic crystallites [34]. Although the reason for the presence of the high temperature phase γ-Fe at ambient temperature is unclear, it is believed that it is related to the formation of turbostratic crystallites.

In the XRD profiles of the Ni-catalyzed carbon samples, peaks corresponding to metallic Ni were detected at $2\theta = 44.4°$ and 51.8°. As the catalyst content increased, the peaks from α-Fe, γ-Fe, and Ni became narrower and more pronounced.
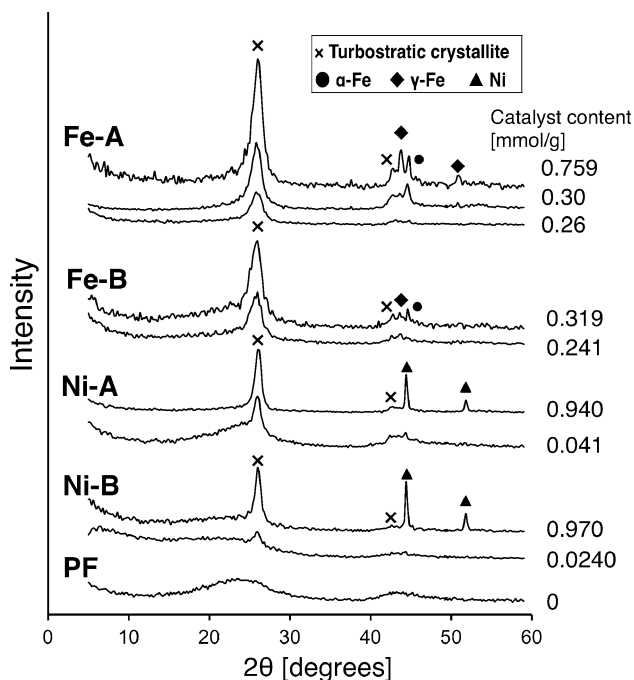
The PF sample formed without catalyst possessed a typical amorphous structure [8]. Doping with Fe and Ni resulted in the formation of carbon aggregates, which consisted of turbostratic crystallites (Fig. 2). In our previous report [8], we observed the morphologies of carbon aggregates using scanning electron microscopy. Carbon species formed using Fe- and Ni-based catalysts possessed whisker and block morphologies, respectively. TEM observation revealed that each whisker and block consisted of tube-like and coil-like structures, respectively. In this study, the structure of the carbon aggregate in the Fe-containing carbon materials depended significantly on the mixing method. Sample 0.26 Fe-A exhibited a cup-stacked structure (Fig. 2a), while 0.241 Fe-B possessed a thin tube-like structure (Fig. 2b). Conversely, similar coil-like structures were found in the carbons containing Ni irrespective of the mixing method (Fig. 2c, d). Therefore, the type of carbon aggregate formed can be influenced by the choice of catalyst and mixing method.

As we showed previously [8], Fe- and Ni-containing carbon samples exhibited N_2 adsorption/desorption isotherms with a hysteresis loop, which indicates the existence of mesopores. The hysteresis loops became more pronounced as the catalyst content increased. This means that the number of mesopores increased with the catalyst content. Recalling that higher catalyst content also resulted in increased amount of turbostratic crystallites (Fig. 1), the increase in mesopores seems to be related to the formation of turbostratic crystallites. Although a previous study also mentioned this relationship [35], it did not provide experimental evidence. Clarification of the relationship between mesopores and turbostratic crystallites necessitates a quantitative discussion. Thus, the amount of mesopores and turbostratic crystallites in the samples was estimated as follows. The mesopore surface area was calculated using the BJH method. The amount of turbostratic crystallites (F_{TS}) was estimated from the XRD profile using the same approach as Ozaki et al. [36]. As shown in Fig. 1, the Fe- and Ni-containing carbon samples showed a conjoined (002) diffraction peak at around 26°, which then separated into a sharp peak and a broad peak. The sharp peak was attributed to the formation of turbostratic crystallites. F_{TS} is the ratio of the area of the sharp peak to the total area of the (002) region. The standard deviation associated with the estimation of F_{TS} is 0.7.

Figure 3 shows the relationship between mesopore surface area and F_{TS}. The mesopore surface area increased proportionally with F_{TS}. This clearly demonstrates that the increase in mesopores is related to the formation of turbostratic crystallites. Note that three lines of best fit can be drawn for the Fe-A, Fe-B, and Ni-A and B samples. As seen in Fig. 2, the obtained carbon samples formed three different types of carbon aggregate. Cup-stacked and thin
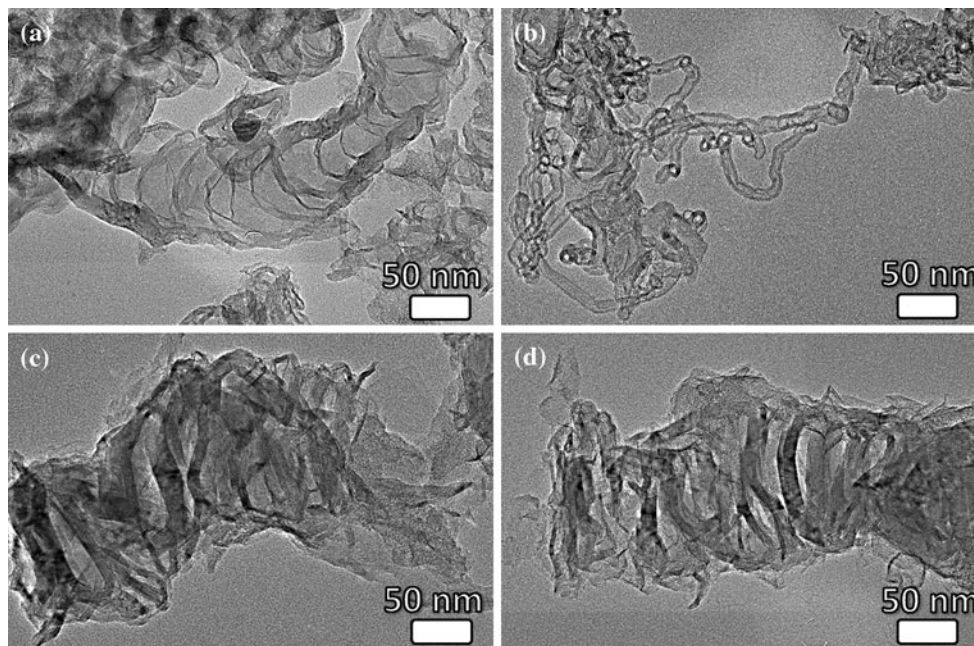

Fig. 1 XRD profiles of Fe- and Ni-containing carbons and PF. Fe and Ni contents (mmol/g) are shown on the right hand side of each profile

Fig. 2 TEM observations of tube-like aggregates in samples 0.26 Fe-A (**a**) and 0.241 Fe-B (**b**), and coil-like aggregates in 0.940 Ni-A (**c**) and 0.970 Ni-B (**d**)
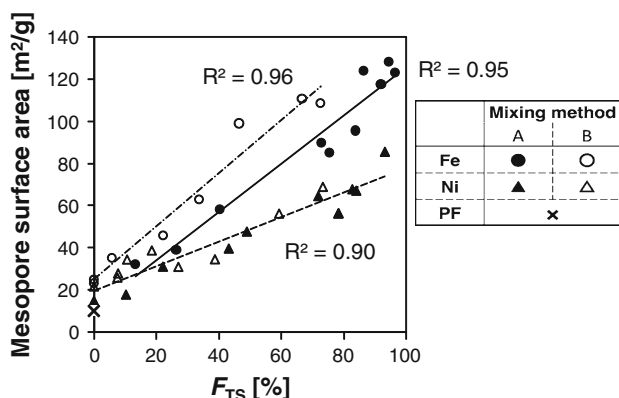

Fig. 3 Relationship between mesopore surface area and the amount of turbostratic crystallites (F_{TS}) in carbon samples produced with and without Fe or Ni catalyst

tube-like structures were found in samples Fe-A and Fe-B, while coil-like structures were observed for samples Ni-A and B. These results suggest that the type of carbon aggregate present also affects the mesopore surface area. Nonetheless, the mesopore surface area was changed predominantly by the amount of turbostratic crystallites present. Thus, it is deduced that the mesopore surface consists of turbostratic crystallites, namely, that mesopores in Ts-carbon are probably surrounded by turbostratic crystallites.

The finding that the mesopore surface area is affected by the amount of turbostratic crystallites in a sample led to subsequent experiments investigating the influence of the size of turbostratic crystallites on the mesoporous structure

of Ts-carbon samples. To gauge the size of turbostratic crystallites, L_c was estimated. This study was also conducted to investigate the relationship between the sizes of the turbostratic crystallites and catalyst particles. Thus, the size of the catalyst particles dispersed in Ts-carbon was estimated by both TEM and XRD. The particle size distribution of Fe and Ni in the 0.26 Fe-A and 0.970 Ni-B samples, respectively, were obtained from TEM observations (Fig. 4). The size of the Fe particles ranges from 10 to 40 nm in 0.26 Fe-A, although most were in the 10–30 nm range. On the other hand, 0.970 Ni-B exhibits a wider size distribution of Ni particles. Ni particles with diameters of more than 100 nm were also observed by Hatori et al. in Ni-catalyzed carbon [11]. The pinnacle of the Ni particle size distribution peak is also shifted to 30–40 nm, which is
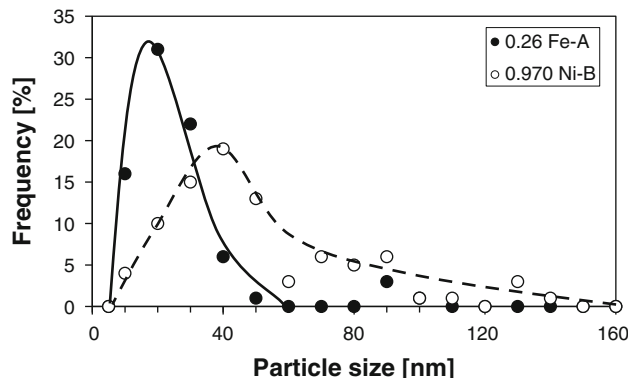

Fig. 4 Particle size distributions for Fe and Ni obtained from TEM micrographs of the 0.26 Fe-A and 0.970 Ni-B samples, respectively

larger than that of Fe. Comparing the Fe- and Ni-catalyzed carbon samples, Ni tends to form larger particles than Fe. In addition to TEM, XRD was also used to estimate the sizes of the Fe and Ni catalyst particles (L_{cat}), which were determined from the full width at half-maximum (FWHM) of the α-Fe (110) and Ni (111) diffraction peaks, respectively, using the Scherrer equation following the same approach as previously reported [10, 11, 16, 19, 24, 25, 37]. The L_{cat} values for samples 0.26 Fe-A and 0.970 Ni-B are 15 and 31 nm, respectively. These values are consistent with the values obtained for the peak tops of the particle size distributions by TEM observations. L_{cat} represents the most common size of catalyst particle in Ts-carbon. Thus, the relationship between the size of turbostratic crystallite and catalyst particle is discussed using L_{cat}.

Figure 5a shows the influence of the content of catalyst in the sample on the L_c of the turbostratic crystallites. While L_c for the Ni-containing carbon samples increased linearly with increasing catalyst content, the L_c in the Fe-containing carbon samples remained constant until the Fe content reaches 0.10 mmol/g. Further addition of Fe catalyst caused L_c to increase. Figure 5b shows the change in L_{cat} with catalyst content. Together with α-Fe, some Fe-catalyzed samples showed a diffraction peak consistent with γ-Fe (Fig. 1). Therefore, the L_{cat} for γ-Fe was also determined from the FWHM of the γ-Fe (111) diffraction peak using the Scherrer equation. The changes in L_{cat} are similar to those of L_c as the catalyst content increases. The

Ni-containing carbon samples showed a linear increase in L_{cat} with Ni content, while L_{cat} of α-Fe and γ-Fe increased linearly when the Fe content exceeded 0.1 mmol/g. L_{cat} values for Fe contents less than 0.07 mmol/g could not be estimated because of the detection limit of XRD. The increase in L_c appears to be related to the increase in L_{cat}.

To obtain more a detailed insight into the effect of catalyst size, L_c was plotted against L_{cat} (Fig. 6). For the Ni-containing carbon samples, L_c increased proportionally with L_{cat} (Fig. 6a). For the carbon samples produced using an Fe catalyst, L_c also increased with L_{cat} calculated from the α-Fe and γ-Fe diffraction peaks. However, the line of best fit for γ-Fe possessed a comparatively better R^2 value than that for α-Fe. These results demonstrate that the catalytic formation of turbostratic crystallites is probably related to γ-Fe rather than α-Fe. It is suggested that under the conditions used, γ-Fe possessed higher catalytic activity for forming turbostratic crystallites than α-Fe. On the other hand, Anton [38] reported the activity of α-Fe. Although the catalytic activity of α-Fe was not determined in this study, it is notable that the size of the catalyst particles is a crucial factor in determining the size of the turbostratic crystallites formed.

As inferred above, the mesopores in Ts-carbon most likely exist among turbostratic crystallites. Thus, the mesopore surrounded by turbostratic crystallites is expected to be influenced by the size of the turbostratic crystallites. The size distributions of mesopores in the Fe- and Ni-containing carbon samples with various L_c values were calculated by the BJH method (Fig. 7). Carbon samples with smaller L_c contained smaller mesopores of around 2 nm. As L_c increased, pores around 3–20 nm developed. As a consequence of the increased mesopore size, the mesopore volume increased. These results suggest that the size and volume of mesopores in Ts-carbon are related to the development of turbostratic crystallites. To gauge this quantitatively, the mesopore volume was plotted against L_c (Fig. 8). The mesopore volume increased linearly with L_c in the Fe- and Ni-containing carbon samples. Note that the mesopore volume and L_c for Fe-A and Fe-B can be approximately expressed by the same linear equation, even though Fe-A and Fe-B contain different types of carbon aggregates (Fig. 2a, b). These results suggest that the mesopore volume in Ts-carbon is related to the size of turbostratic crystallites rather than the type of carbon aggregate. However, for the Fe- and Ni-containing carbon samples, the relationship between L_c and mesopore volume was not expressed by the same equation. There should be inherent structural differences in the mesopores formed by turbostratic crystallites produced by Fe or Ni catalysts. Although the origin of the structural difference is not clear, the mesopore size and volume depended predominantly on L_c. Thus, it is concluded that the control over the size and
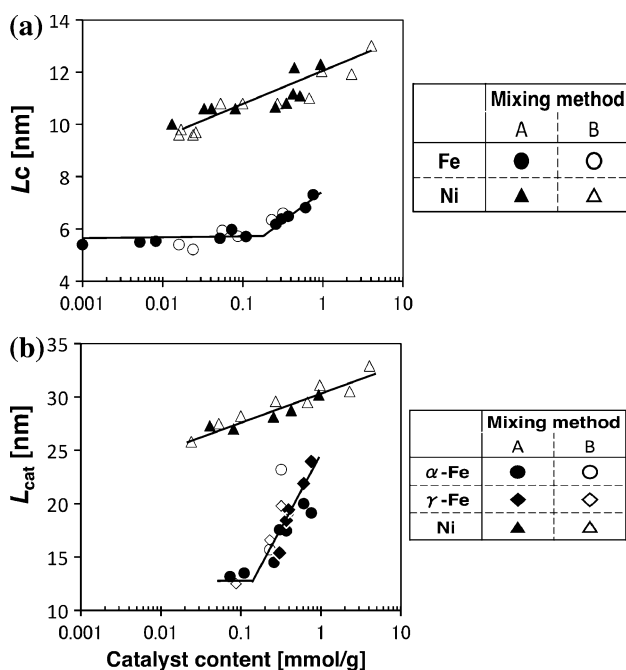

Fig. 5 Change in the XRD parameters of Fe- and Ni-containing carbon samples as a function of the catalyst content. **a** Size of turbostratic crystallites (L_c); **b** size of catalyst particles (L_{cat}) for α-Fe, γ-Fe, and Ni

Fig. 6 Relationships between L_c and L_{cat} for Ni (**a**) α-Fe (**b**), and γ-Fe (**c**). *Closed symbols* mixing method A; *open symbols* mixing method B
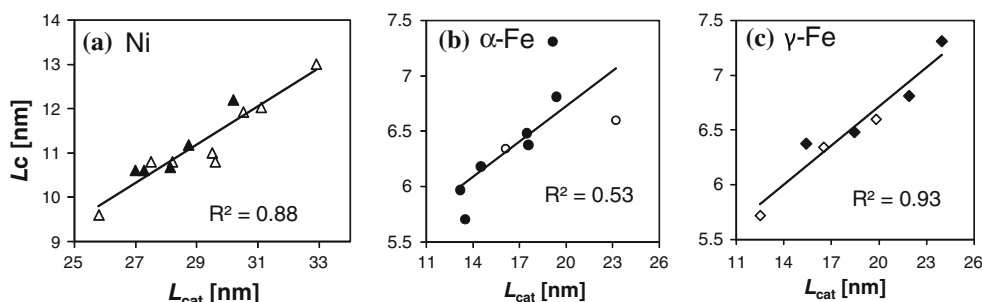
Fig. 7 Change of mesopore size distribution as L_c increases in Fe-containing (**a**) and Ni-containing (**b**) carbon samples. PF, which does not contain turbostratic crystallites, is shown as a reference. L_c values for the turbostratic crystallites are shown on each curve
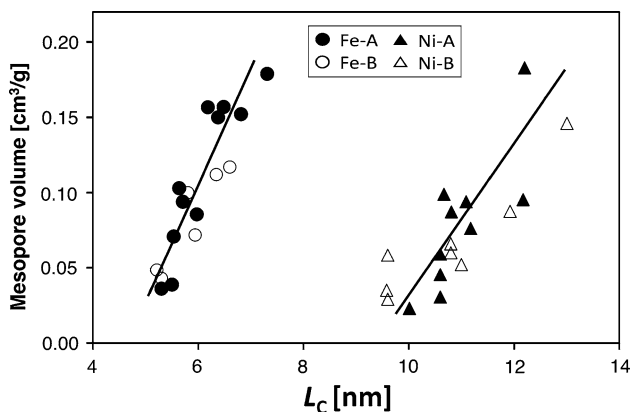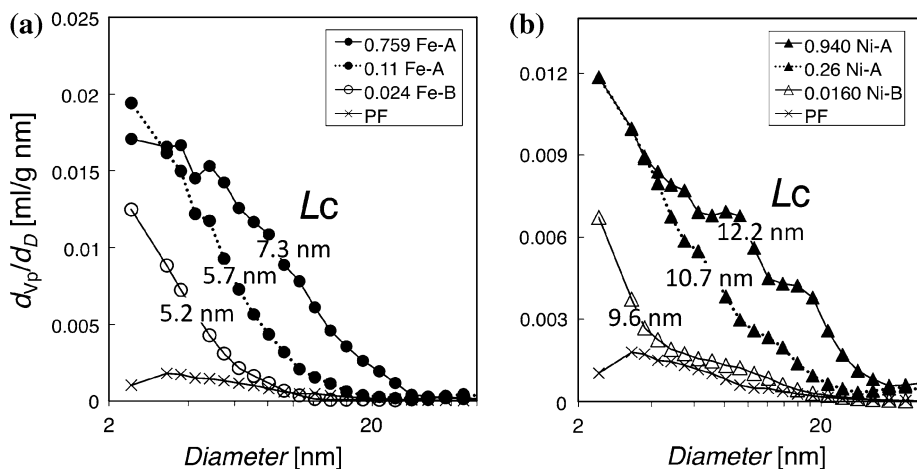
Fig. 8 Relationship between mesopore volume and L_c of Ts-carbon formed using various amounts of Fe or Ni catalyst. All samples were carbonized at a fixed temperature of 1000 °C for 1 h

volume of mesopores in Ts-carbon is made possible by altering the size of turbostratic crystallites, which can be achieved simply by changing the content of metal catalyst.

Conclusions

In conclusion, a technique has been developed to control the mesoporous structure and size of carbon crystallites in Ts-carbon. Mesopores and turbostratic crystallites are

formed in Ts-carbon samples produced from Fe- or Ni-doped phenolic resin that is treated at 1000 °C. The turbostratic crystallites assemble to form different carbon aggregates depending on the catalyst and the mixing method used. Our results clearly demonstrate that the surface area of the mesopores is predominantly related to the amount of turbostratic crystallites present rather than the type of the carbon aggregate. Thus, it is proposed that the mesopores in Ts-carbon are surrounded by turbostratic crystallites.

The effect of the size of catalyst particles dispersed in Ts-carbon on the size of turbostratic crystallites was clarified. L_c increases proportionally with L_{cat} for γ-Fe and Ni, indicating that γ-Fe and Ni possess catalytic activity for the formation of turbostratic crystallites. Our results suggest that the size of the catalyst particles is a crucial factor in determining the size of turbostratic crystallites.

Increasing L_c increases the size and volume of the mesopores in Ts-carbon linearly, irrespective of the type of carbon aggregate. Therefore, altering the size of turbostratic crystallites is an effective method for controlling the size and volume of mesopores in Ts-carbon.

The techniques presented in this study will allow the production of Ts-carbon with tailored porous and crystallite structures. These materials promise high catalytic activity and selectivity. A study of the microporous structures in Ts-carbon is in progress.

References

1. Nagano S, Tamon H, Adzumi T, Nakagawa K, Suzuki T (2000) Carbon 38:915
2. Yang JB, Ling LC, Liu L, Kang FY, Huang ZH, Wu H (2002) Carbon 40:911
3. Tamai H, Kakii T, Hirota Y, Kumamoto T, Yasuda H (1996) Chem Mater 8:454
4. Shiraishi S, Kurihara H, Oya A (2001) Electrochemistry 69(6):440
5. Marsh H, Rodriguez-Reinoso F (2006) Activated carbon. Elsevier Science, New York
6. Ariyadejwanich P, Tanthapanichakoon W, Nakagawa K, Mukai SR, Tamon H (2003) Carbon 41:157
7. Ryu Z, Zheng J, Wang M (1998) Carbon 36(4):427
8. Inomata K, Otake Y (2009) J Mater Sci 44:4200. doi:10.1007/s10853-009-3560-2
9. Wang X, Liu J, Li Z (2009) J Non-Cryst Solids 355:72
10. Maldonado-Hodar FJ, Moreno-Castilla C, Rivera-Utrilla J, Hanzawa Y, Yamada Y (2000) Langmuir 16:4367
11. Hatori H, Kobayashi T, Hishiki S, Yamada Y, Matsuno S, Nishio T (2002) Synth Metals 125:183
12. Zhao M, Song H, Chen X, Lian W (2007) Acta Mater 55:6144
13. Oka H, Inagaki M, Kaburagi Y, Hishiyama Y (1999) Solid State Ion 121:157
14. Park SH, Jo SM, Kim DY, Lee WS, Kim BC (2005) Synth Metals 150:265
15. Ozaki J, Yoshimoto Y, Oya A, Takarada T, Kuzunetsov VV, Ismagilov ZR (2001) Carbon 39:1611
16. Sevilla M, Sanchis C, Valdes-Solis T, Morallon E, Fuertes AB (2008) Carbon 46:931
17. Sevilla M, Lota G, Fuertes AB (2007) J Power Sour 171:546
18. Ozaki J, Nozawa K, Yamada K, Uchiyama Y, Yoshimoto Y, Furuichi A, Yokoyama T, Oya A, Brown LJ, Cashion JD (2006) J Appl Electrochem 36:239
19. Sevilla M, Fuertes AB (2009) Mater Chem Phys 113:208
20. Oya A, Inoue E, Otani S, Marsh H (1981) Fuel 60:1099
21. Oya A, Yutaka A, Otani S (1980) Fuel 59:595
22. Bin YZ, Oishi K, Koganemaru A, Zhu D, Matsuo M (2005) Carbon 43:1617
23. Otani S, Oya A, Akagami J (1975) Carbon 13:353
24. Kaburagi Y, Hishiyama Y, Oka H, Inagaki M (2001) Carbon 39:593
25. Kaburagi Y, Hatori H, Yoshida A, Hishiyama Y, Inagaki M (2002) Synth Metals 125:171
26. Oya A, Mochizuki M, Otani S, Tomizuka I (1979) Carbon 17:71
27. Oya A, Otani S (1978) Carbon 16:153
28. Oya A, Marsh H (1982) J Mater Sci 17:309. doi:10.1007/BF00591464
29. Iwashita N, Park CR, Fujimoto H, Shiraishi M, Inagaki M (2004) Carbon 42:701
30. Fujimoto H (2003) Tanso 206:2
31. Barrett EP, Joyner LG, Halenda PP (1951) J Am Chem Soc 73(1):373
32. Benz MG, Elliott JF (1961) Trans AIME 221:323
33. Ozaki J, Mitsui M, Nishiyama Y, Cashion JD, Brown LJ (1998) Chem Mater 10:3386
34. Derbyshire FJ, Presland AEB, Trimm DL (1975) Carbon 13:111
35. Lu AH, Li WC, Salabas EL, Spliethoff B, Schuth F (2006) Chem Mater 18:2086
36. Ozaki J, Nozawa K, Oya A (1998) Chem Lett 7:573
37. Laskoski M, Keller TM, Oadri SB (2007) Carbon 45:443
38. Anton R (2009) Carbon 47:856